

PACS numbers: 47.61.Ne, 64.70.D-, 65.40.De, 66.30.Xj, 66.70.Hk, 81.70.Pg, 88.80.F-

Experimental Investigation of the Effect of Expanded Graphite on the Thermophysical Properties and the Heating and Cooling Rates of Paraffin Wax in Capsule of Thermal-Energy Storage System

Vitaly Zhelezny¹, Olga Khliyeva², Yana Hlek¹, Oleksiy Paskal¹,
Dmytro Ivchenko¹, and Mykola Lapardin¹

¹*Odesa National Academy of Food Technologies,
1/3, Dvoryanska Str.,
UA-65082 Odesa, Ukraine*

²*National University 'Odesa Maritime Academy',
8, Didrikhson Str.,
UA-65029 Odesa, Ukraine*

Expanded graphite (EG) is a promising component to improve the properties of the phase-change materials (PCMs) for thermal-energy storage (TES) systems. The experimental study of the EG effect on the thermophysical properties of the paraffin wax (PW) and the heating and cooling rates in experimental cell, which is a model of the TES system capsule, is performed. Two samples of the PW-based composite PCM are prepared using different methods: PW/EG#1 and PW/EG#2 containing $0.178 \text{ g}\cdot\text{g}^{-1}$ and $0.111 \text{ g}\cdot\text{g}^{-1}$ of EG, respectively. The evacuation during the preparing procedure contributes to more full filling of the EG pores with PW and lower EG content in PCM. The EG presence in PW/EG#1 and PW/EG#2 contributes to the thermal-conductivity enhancement by 800% and 640%, respectively, in the range under the PW melting point (53.5°C), and by 930% and 740%, respectively, in the range above 53.5°C . Duration of the melting and heating from 48°C to 59°C of PW within the capsule is found to be of 12.0 min. *vs.* 1.1 min. and 1.4 min. for the PW/EG#1 and PW/EG#2, respectively. The heating duration from 30°C to 40°C of PW is of 7.7 min. *vs.* 1.6 min. for both samples. The 'jump' of the density and thermal-conductivity values are not observed for the PW containing EG during transition of the PW melting point. It will contribute to both the faster smoothing of the temperature field in the capsules of the TES systems containing such PCM and the absence of the linear extensions of capsules.

Терморозширений графіт (ТРГ) є перспективним компонентом для по-

ліпшення властивостей матеріалів з фазовим переходом (МФП) з метою використання їх у термоакумуляторах. Проведено експериментальне дослідження впливу ТРГ на теплофізичні властивості парафіну та швидкості його нагрівання й охолодження у експериментальній комірці, яка є моделлю капсули термоакумулятора. З використанням різних технологій було виготовлено два зразки композитного МФП на основі парафіну, — PW/EG#1 і PW/EG#2, — із вмістом $0,178 \text{ г}\cdot\text{г}^{-1}$ і $0,111 \text{ г}\cdot\text{г}^{-1}$ ТРГ відповідно. Показано, що вакуумування під час приготування сприяє більш повному заповненню парафіном пор ТРГ та меншому вмісту ТРГ в МФП. Наявність ТРГ в PW/EG#1 і PW/EG#2 сприяла підвищенню теплопровідності на 800% і 640% відповідно за температури нижче точки топлення парафіну ($53,5^\circ\text{C}$). Підвищення теплопровідності для PW/EG#1 і PW/EG#2 в діапазоні вище температури $53,5^\circ\text{C}$ становило 930% і 740% відповідно. Тривалість нагрівання та топлення від 48°C до 59°C зразків у капсулі становила 12,0 хв. для парафіну проти 1,1 хв. і 1,4 хв. для PW/EG#1 і PW/EG#2 відповідно. Тривалість нагріву парафіну від 30°C до 40°C становила 7,7 хв. проти 1,6 хв. для обох зразків. Для МФП із вмістом ТРГ зі збільшенням температури вище точки топлення парафіну не спостерігався «стрибок» густини та теплопровідності. Це сприятиме більш швидкому вирівнюванню температурного поля в капсулах термоакумуляторів, що заповнені дослідженими МФП, та відсутності лінійних розширень капсул.

Key words: industrial paraffin wax, expanded graphite, density, thermal conductivity, heating and cooling rates, model of the capsule of thermal-energy storage system.

Ключові слова: технічний парафін, терморозширений графіт, густина, теплопровідність, швидкості нагріву й охолодження, модель капсули для термоакумуляторної системи.

(Received 28 April, 2022)

1. INTRODUCTION

Carbon nanomaterials are one of the most promising components used to improve the thermal conductivity of the thermal storage phase-change materials (PCMs) due to their chemical stability, low corrosion activity, and high thermal conductivity [1]. However, applying carbon nanomaterials, such as fullerenes and carbon nanotube, has several disadvantages. The first problem is their high cost. The second problem is their low stability to clusterization and precipitation under composite PCM cyclic melting/solidification in the TES system. At the same time, mentioned problems are not typical in case of using the rational fraction of the expanded graphite (EG) as an additive to the PCM. Expanded graphite can be considered as one of the promising components for the composite PCMs

[2]. The main advantages of the EG are its inexpensive and high thermal conductivity.

The latent heat thermal energy storage (TES) systems are attractive in comparison with the sensible heat thermal-energy storage due to inherent the high storage density with small temperature swings and isothermal features during the charging/discharging periods. However, main disadvantages of the TES are the low thermal conductivity for the widespread PCMs, such as paraffin wax (PW), as well as the higher cost per one joule of the energy storage. To overcome this drawback, various approaches are studied now, for example, the additives of the high-thermal-conductivity carbon nanomaterials into the PCM [3, 4]. Another complication of the implementation in practice of the latent heat TES system is concerned with the necessity of the additional analysis for the heat-transfer processes in elements of the TES system containing promising PCMs.

The thermal conductivity of the EG is varied in the range 4–70 $\text{W}\cdot\text{m}^{-1}\cdot\text{K}^{-1}$ [5], 2–90 $\text{W}\cdot\text{m}^{-1}\cdot\text{K}^{-1}$ [6], or about 100 $\text{W}\cdot\text{m}^{-1}\cdot\text{K}^{-1}$ [7]. Therefore, it is expected a significant increase in the thermal conductivity of composite PCMs containing EG. The FireCarb TEG-315 and FireCarb TEG-160 were used as EG (2, 4, and 6 wt.%), and PW with melting temperature of 53–57°C was applied as the PCM in the study [8]. The thermal conductivity of composite PCM with 6 wt.% of TEG-315 and TEG-160 was determined to be of 0.977 $\text{W}\cdot\text{m}^{-1}\cdot\text{K}^{-1}$ and 1.263 $\text{W}\cdot\text{m}^{-1}\cdot\text{K}^{-1}$, respectively, *vs.* 0.258 $\text{W}\cdot\text{m}^{-1}\cdot\text{K}^{-1}$ for the pure PW. An experimental study of the thermal conductivity for the PW/EG containing the EG particles of various sizes (15–25 wt.% of EG) was performed in Ref. [9]. The thermal conductivity of PW/EG with particles of 400 μm in average diameter shows an enhancement by 1360–1695% *vs.* 90–340% increment in the case of particles with an average diameter less than 1 μm . A greater increase in thermal conductivity of EG/PW (88.7% vol. of PW) was shown in Ref. [10]: 20.8 $\text{W}\cdot\text{m}^{-1}\cdot\text{K}^{-1}$ at 60°C, which is almost 70 times more than for the pure PW. The analysis of studies [7–12] showed a significant inequality in obtained effects of EG on thermal conductivity and the efficiency of heat transfer in composite PCMs.

The standard preparing method for the composite PCMs containing EG has not been developed yet. It may explain a significant variation in obtained experimental data on the thermal conductivity reported by different researchers for these composites. Analysis of some studies [2, 8] shows that mixing of the PW and EG without any additional treatment does not allow to obtain composite PCM with appropriate properties for utilization in the TES systems.

Based on the performed analysis, it was decided to focus on evaluating the feasibility of using the EG as additives to the PW to

create the composite PCM for the TES systems. Review of the experimental studies has demonstrated that utilizing the EG as an additive to the PCMs contributes to an increase in the thermal conductivity, but a decrease in the heat capacity of the composite PCMs. At the same time, compromise between the high thermal conductivity and large thermal capacity for PCMs is critically significant for development of the TES systems [13]. The TES system performance cannot be characterized by the latent heat and thermal conductivity values of the PCM only. The temperature–time curve for the capsule with the PCM during the heating and cooling processes is practically important criterion for the assessment of the TES system performance. Thus, analysis of both the thermophysical properties of PCMs and the rate of temperature changing during their heating and cooling in the model of the TES capsule can be used as a comprehensive approach to the assessment of the PCMs' effectiveness considering their method of preparation.

This paper is dedicated to the experimental study of the effect of the EG on PW thermophysical properties and rate of changing its temperature during heating (charging) and cooling (discharging). A feature of the study is utilizing the experimental cell, which is a model of the TES system capsule. The following tasks have been examined:

- to develop the method of the preparing the composite thermal storage PCMs containing EG;
- to perform an experimental study of the thermophysical properties of the PW-based PCMs containing EG;
- to investigate experimentally the effect of the EG in PW on the rate of changing its temperature during heating and cooling in two modes: with phase transition solid–liquid and without phase transition.

2. MATERIALS AND RESEARCH METHODS

The following materials have been used to prepare the investigated samples:

- paraffin wax (industrial grade T-3, melting temperature 53.5°C, made in Poland);
- expanded graphite (highly conductive expanded graphite powder GFG200, supplier the SGL Sigratherm, Germany, purity not less than 95 wt.%, D_{50} determined by sieve analysis—200 μm , powder bulk density 100 $\text{g}\cdot\text{sm}^{-3}$).

The image of pristine sample of the EG is presented in Fig. 1.

The densities of the PW in the temperature range from 0 to 46°C and PW/EG#1 in the temperature range from 15 to 75°C were measured by pycnometer method for the solid phase with additional



Fig. 1. Image of the powder of EG in the pycnometer.

filling of the pycnometer by distilled water. The density of the PW liquid phase in the temperature range from 55 to 72°C was measured by pycnometer method. The measurement of the density of samples was performed as follows:

- without previously sample treatment for the PW in liquid and solid phases;
- with previously evacuation at 0.1 bar (for removing dissolved air) for the PW, PW/EG#1, and PW/EG#2 in the solid phase.

For characterization of the obtained composite PCM (completeness of filling of the EG pores with PW), the porosity of the samples (volume fraction of pores filled with air) was calculated as follows:

$$\varepsilon = 1 - \rho_{PW/EG\ exp} / \rho_{PW/EG\ add} , \quad (1)$$

where $\rho_{PW/EG\ exp}$ and $\rho_{PW/EG\ add}$ are the densities of the composite PCM, which were measured and calculated by additivity rule, respectively.

The ‘real’ EG density (without pores) was assumed equal to 2.20 g·sm⁻³. This value was taken based on data reported elsewhere: x-ray density of the graphite—2.24 g·sm⁻³ [14, 15], the real density of EG as filler—2.25 g·sm⁻³ [16], true density of the EG by SGL Carbon (the same EG purchaser as in presented study)—2.190 g·sm⁻³ [17].

Thermal conductivity measurements for the solid samples were performed using a precision devise Hot Disk TPS 2500 S (according to standards ISO 22007-2) with sensor All Kapton ($d = 2$ mm) meant for isotropic samples. Instrumental uncertainty does not exceed 5%. The measurements were performed for various combinations of

the samples for the same PCM type (two samples for one measurement) in the temperature range from 20 to 70°C for the PW/EG#1 and PW/EG#2 samples and at the one temperature of 22°C for the pure PW. The obtained values of the thermal conductivity were averaged for each PCM type.

The thermal conductivity of the liquid PW in the temperature range 55–77°C was examined using measuring cell that implements the transient hot-wire method [18]. Instrumental uncertainty in that experiment does not exceed 2.0%.

The results of caloric-properties' measurement for the PW and PW/EG#2 are presented in Ref. [19].

Experimental setup and measurements method for investigation the temperature–time curve for the capsule with the PCM sample during heating and cooling are described in detail in Ref. [20]. The experimental cell made from copper was considered as model of the capsule for the TES system (Fig. 2). An absolute thermocouple was installed in the middle of the height of the cell on its axis. Thermocouple readings were recorded by Pisotest M3500A multimeter. Uncertainty of the temperature measurement was evaluated as 0.5°C.

Two modes were examined for heating and cooling of the PCM samples:

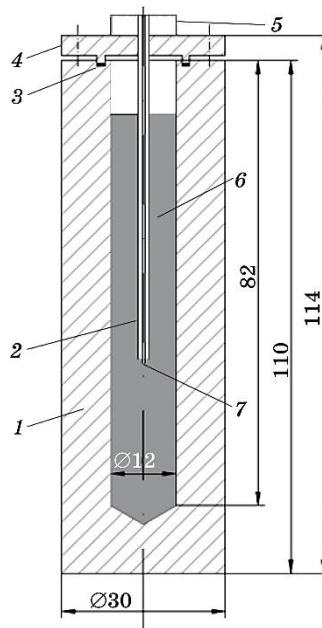


Fig. 2. Scheme of the measuring cell: 1—copper shell; 2—thin-walled capillaries; 3—sealing gasket; 4—cover; 5—tube; 6—sample; 7—thermocouple.

- 1) *the mode with a phase transition*—the measuring cell filled with the PCM sample was heated from 48 to 59°C in the centre of the cell after dipping into the water of 59°C, and after that, the cell was cooled from 59 to 48°C after dipping into the water of 48°C;
- 2) *the mode without phase transition*—the measuring cell filled with the PCM sample was heated from 30 to 40°C in the centre of the cell after dipping into the water of 40°C, and after that, the cell was cooled from 40 to 30°C after dipping into the water of 30°C.

The experiment was conducted under convection boundary conditions (the constant heat-transfer coefficient from cell to water in the thermostat). The thermal resistances of both the measuring cell wall and the heat transfer from water to the wall were insignificant compared to the thermal resistance of the PCM layer in the cell.

3. PREPARING METHODS OF OBJECT OF STUDY

Two approaches to preparing the composite PCM containing EG were used. The first method is based on the pristine EG mixing with melted PW (70–75°C) and mechanical stirring of the components. No previous treatment of components was implemented in this case. The obtained sample denotes in the figures and text as the PW/EG#1. The second method is based on EG heating (up to 700°C) with evacuation (0.1 bar of abs. pressure) for 15 min., followed by mixing preevacuated melted PW (70–75°C) and evacuation of the obtained composite PCM at 65°C for 30 min. The obtained sample denotes in the figures and text as the PW/EG#2.

A rapid separation into the pure PW and PW containing EG with a clear interface was observed for two hours after preparing and keeping both samples at 70–75°C (Fig. 3). It was assumed that stable and almost filled by the PW structure of EG has been obtained in the precipitated layer. After crystallization of the PW/EG, the upper pure PW was carefully removed and weighed. All weighing was performed using the Model GR 300 electronic balance with an instrument uncertainty of 0.5 mg.

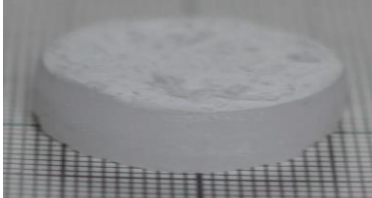
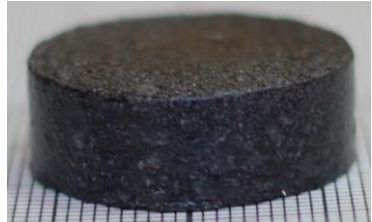

The images of PCM samples in the form of pellets and the mass fractions of EG in the PW/EG#1 and PW/EG#2 samples, which were obtained after removing and weighing the upper layer of pure PW, are presented in Table.

The sample PW/EG#1 prepared without preliminary evacuation of the pristine components was characterized by high mass fraction of the EG. The PW/EG#1 contains 0.178 g·g⁻¹ of EG *vs.* 0.111 g·g⁻¹ for PW/EG#2 (Table). High content of the EG in PW/EG#1 indirectly confirms the presence in sample of the volume zones containing only EG with air in pores. The studies [8, 21–23] demonstrated that the ‘optimal’ mass fraction of EG in PW may vary in range 7–



Fig. 3. Images of the PW/EG#2 sample (a clear interface between PW/EG#2 sample and pure PW after preparation).

TABLE. Characteristics of the PCM samples.

Labelling in the figures and text	EG mass fraction, $\text{g}\cdot\text{g}^{-1}$	Images of the composite thermal storage PCM
PW	0	
PW/EG#1	0.178	
PW/EG#2	0.111	

10 wt.%. The low EG content can lead to its precipitation in the PCM, but high EG content contributes the anisotropic thermal conductivity and low enthalpy of melting. The problem of choice the 'optimal' EG mass fraction requires additional examination.

It was also observed that the PW pellets poorly hold up their original shape with sharp edges during preservation, when ambient temperature fluctuated in the range 20–35°C in contrast to the PW/EG#1 and PW/EG#2 pellets (Table presents sample images after their preservation for one month at the temperature up to 35°C). Keeping the shape by composites PW/EG#1 and PW/EG#2, when the PW is softened, can be useful from a practical point of view. The phase transition will not be followed by a significant (approximately 10% [24] as for PW) change in the volume of the composite PCMs containing the EG. This simplifies the design of PCM capsules by the absence of the compensators for their linear size-changing [25]. The additional advantage of the obtained composites PCMs is a decrease in the PW leakage at the temperatures above the melting point [9].

4. EXPERIMENTAL RESULTS AND DISCUSSION

4.1. Density and Air Content

The results obtained for the samples' density in the solid and liquid phases are presented in Fig. 4.

The measured values of the PW density in the liquid and solid

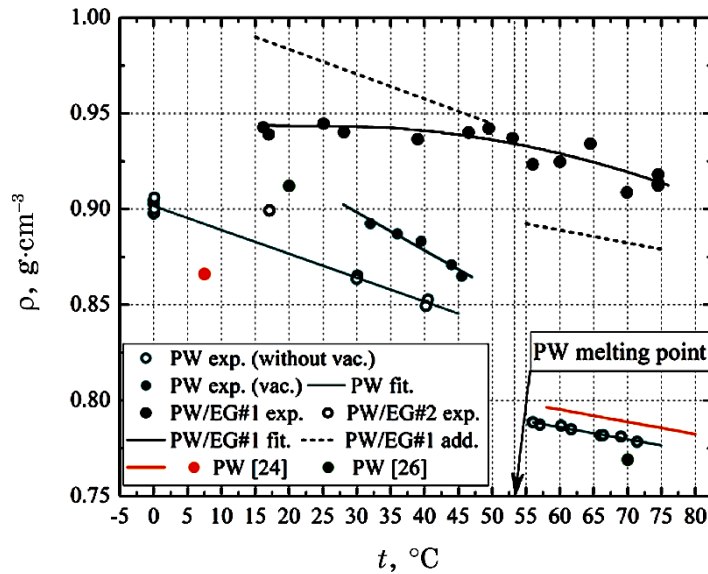


Fig. 4. Temperature dependence of the density for solid and liquid phases for the pure PW, PW/EG#1 and PW/EG#2 as well as for industrial-grade PWs with $t_m=52.0-54.0^{\circ}\text{C}$ [24] and $t_m=48.0-50.0^{\circ}\text{C}$ [26].

phases are in a good agreement with the reference data obtained for industrial PW with close melting temperature (Fig. 4).

The density of solid PW was measured twice: with preliminary evacuation of the samples and without preevacuation. The temperature dependences of the PW density (Fig. 4) obtained by two measurements are almost equidistant with a difference of approximately $0.03 \text{ g}\cdot\text{cm}^{-3}$. This difference can be explained by presence of the dissolved air in the non-preevacuated PW sample.

The 'jump' of the density was not observed for the PW/EG#1 during the transition of the PW melting point. As a result, significant deviations of the density values for the PW/EG#1 calculated by additivity rule and obtained experimentally were found. This fact can be explained as follows. During composite PCM preparation (at the temperature of above 70°C), the EG skeleton with liquid PW between the EG particles and in their pores is formed. The EG skeleton insignificantly changes its volume with temperature decreases. At that, the PW can crystallize under existing conditions with forming the 'loose' structure (that differs from the structure that is formed during crystallization in free volume) or may crack and sucks the air. The mentioned above is also confirmed by deviation of the experimental and calculated data by additivity rule for the density of the PW/EG#1 that is the greater, when temperature is lower. The opposite deviation of the experimental and calculated by additivity data for the PW/EG#1 in the range above the PW melting point ($55\text{--}75^\circ\text{C}$) can be explained by presence of air in the liquid PW during its density measurement, while the measurement of the PW/EG#1 density in the same temperature range was performed after preevacuation.

The porosity (air content) for the samples PW/EG#1 and PW/EG#2 was evaluated at the temperature of 17°C . The calculated value of porosity depends on the temperature (change in the PW crystal structure and PW deaeration can occur with temperature variation). However, the evaluation of PCMs porosity at the one temperature is reasonable to previous analysis of the composite PCM preparing methods.

The calculation results have shown that the fraction of the pores that not filled by PW in the PW/EG#1 sample was of 7.50 vol.% *vs.* 4.75 vol.% for the PW/EG#2 sample. Consequently, utilizing the method with evacuation, the PCM components for sample preparation resulted in a higher filling degree of the EG pores with PW. The greater degree of the EG pores filling by PW may lead to higher thermal conductivity and specific heat capacity of the composite PCM (at equal content of EG).

There are several explanations for relatively high air content in the obtained PCM. Liquid PW may have high dissolved air content

[27–29] that prevents the complete filling of EG pores during composite PCM preparation. In addition, the air is leaked in cracks in the solid PW that formed during its contraction at crystallization [27–30]. To the best knowledge of the authors, there are no studies that denote the investigation of the air content in the PW during preparation and thermophysical-properties' measurements of the PW-based composite PCMs. However, there are studies [27, 28, 31], in which this problem is highlighted. In Ref. [27], it was supposed to melt paraffin under a vacuum and fill the heat sink with it layer-by-layer to ensure the absence of internal voids or air bubbles. In Ref. [28], it was noted that, before the thermal-conductivity measurement, the liquid *n*-octadecane as PCM should be degassed carefully. The probability of further air solving and it leaked in at crystallization during industrial applying of PCMs has no considered in Refs. [27, 28]. In Ref. [31], to address this serious issue connected with the ability of changing the PW properties by dissolved air presence, the choice of a suitable container for PCM was proposed.

4.2. Thermal Conductivity

The results of thermal conductivity measurement for samples in the solid and liquid phases are presented in Fig. 5.

The measured values of the PW thermal conductivity in the liquid and solid phases are in a good agreement with reference data

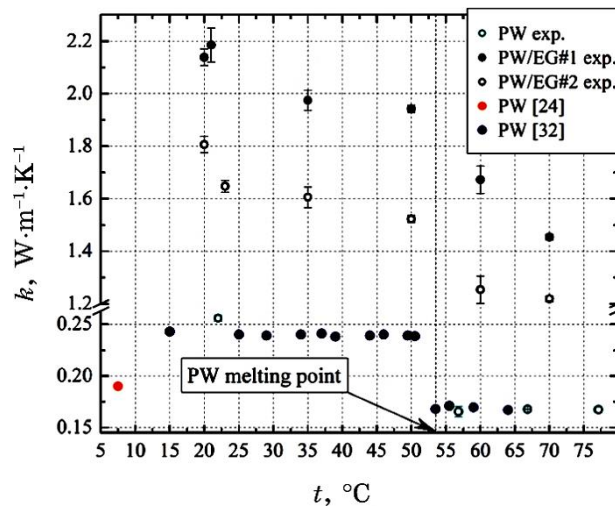


Fig. 5. Temperature dependence of the thermal conductivity for the pure PW, PW/EG#1, and PW/EG#2, as well as for industrial-grade PWs with $t_m = 52.0\text{--}54.0^\circ\text{C}$ [24] and $t_m = 53.0^\circ\text{C}$ [32].

obtained for the industrial PW with close melting temperatures (Fig. 5).

The average value of the thermal conductivity for the solid phase (20–50°C) of PW/EG#1 increased by 800% *vs.* thermal conductivity of pure PW. For the PW/EG#2, the thermal conductivity enhancement was found of about 640%. Enhancement of the thermal conductivity for PW/EG#1 and PW/EG#2 in the range above PW melting point (60–70°C) was of 930% and 740%, respectively, in comparison with the pure PW. The greater effect of the EGG on the thermal conductivity enhancement in the range above PW melting point (60–70°C) *vs.* range 20–50°C can be explained in following manner. Firstly, main mechanism of the heat transfer in the PW/EG is thermal conductivity through the EG skeleton. Thus, the thermal conductivity of the pure PW has insignificant influence on the effective thermal conductivity of the composite PCM. This can explain the absence of a ‘jump’ in the thermal conductivity of PW/EG#1 and PW/EG#2 during the transition through the PW melting point. Secondly, to measure the thermal conductivity of solid and liquid samples, different methods were applied. For pure PW in the liquid phase, the ‘true’ thermal conductivity was measured (at the absence of convection). Another method was used in the temperature range of 60–70°C for the PW/EG#1 and PW/EG#2 samples. The effective thermal conductivity was measured. The contribution of microconvection to the thermal conductivity increasing cannot be excluded in this method (although this contribution is insignificant).

4.3. The Rates of Heating and Cooling

Figure 5 shows the temperature change during the charging (heating) and discharging (cooling) processes in the measuring cell centre. The results for two or three series of measurements for each object of study in all experimental modes are presented. The temperature–time dependence for the pure PW was considered in detail in Ref. [20] and then was used as a baseline characteristic to assess the influence of the EG on the composite PCM heating and cooling rates.

As can be seen from Fig. 6, the PW/EG#1 and PW/EG#2 samples have a significantly higher heating rate compared to pure PW. The melting and heating duration from 48°C to 59°C was determined as of about 12.0 minutes for the sample of pure PW (Fig. 7). For the PW/EG#1 and PW/EG#2 samples, the heating times were significantly lower—of about 1.1 minutes and 1.4 minutes, respectively. The heating rate in the range from 30°C to 40°C was of about 1.6 minutes for both PW/EG#1 and PW/EG#2 samples *vs.*

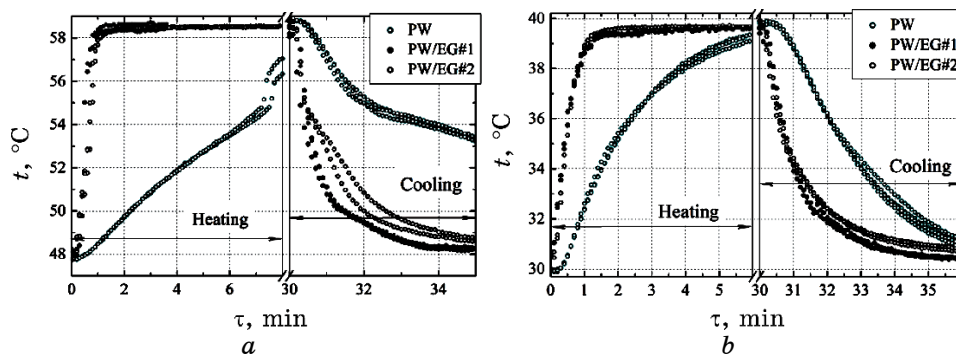


Fig. 6. Time dependence of the temperature of PCM in the centre of the measuring cell: *a*—at the mode with phase transition; *b*—at the mode without phase transition.

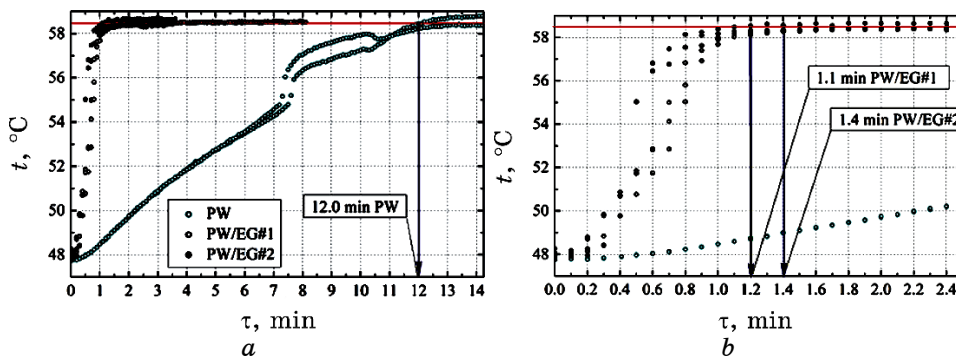


Fig. 7. Determination of the heating time at the mode with phase transition: *a*—for PW; *b*—for PW/EG#1 and PW/EG#2.

7.7 minutes for the pure PW sample (Fig. 8). It was shown that the heating rate due to adding the EG in PW increased by 8.6–10.9 times in the mode with phase transition and in 4.8 times in the mode without phase transition.

The smaller effect of the EG on the heating rate of the PW/EG#1 and PW/EG#2 samples in the mode without the phase transitions *vs.* mode with phase transitions can be explained by the following. The thermal conductivity of the PW liquid phase is less than that of the solid phase (Fig. 5). This difference (even in the presence of convection) contributes to a decrease in the heat-transfer rate in the PW sample in the mode with the phase transition *vs.* mode without phase transition. However, in the PW/EG composite, the heat is transferred through the EG skeleton, and the thermal conductivity of PW has an insignificant effect on the over-

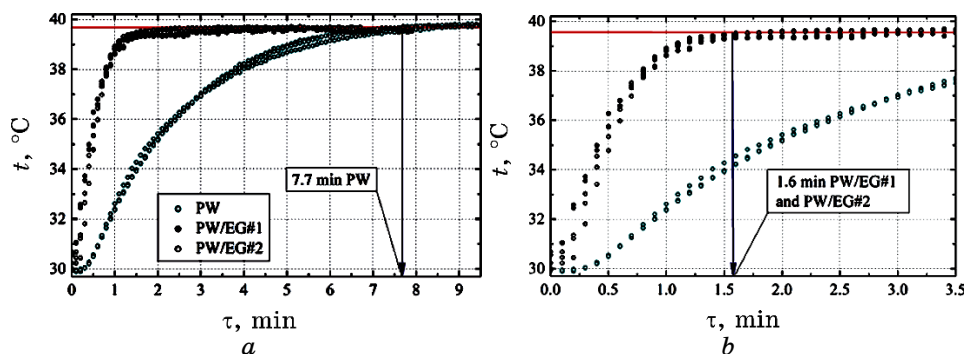


Fig. 8. Determination of the heating time at the mode without phase transition: *a*—for PW; *b*—for PW/EG#1 and PW/EG#2.

all rate of heat transfer. Convection of the liquid PW in composite PW/EG is negligible (due to small size of the EG pores and space between the EG particles as well as the high viscosity of liquid PW [33]).

Heating curves' shape in the mode with a phase transition for the PW and PW/EG is different (Figs. 6, 7). Recorded rapid temperature change (54.5–56°C) for the PW heating is absent for PW containing EG (Fig. 6). This temperature 'jump' for the PW can be explained in following manner. At the reaching the melting point in the centre of the sample, the liquid PW at the top of the cell had an overheated state relative to its melting point. Therefore, after melting the PW in the cell centre, the heat was supplied from the top of the cell to the centre with the currents of the molten PW [20] (Fig. 6). The absence of temperature 'jump' for the samples PW/EG#1 and PW/EG#2 is explained by absence of the bottom-up convective currents of the liquid PW. The thermal conductivity through the EG skeleton and EG granules is a main heat-transfer mechanism. This fact has practical importance, since using the PW/EG as PCM will contribute to the faster smoothing of the temperature field of capsules with PCM that is important for capsules for the TES systems in the form of vertical tubes.

Despite a higher value of thermal conductivity of PW/EG#1 *vs.* PW/EG#2 (Fig. 5), there is no significant difference between the charging and discharging times for capsule with these composite PCM. The obtained effect can be explained as follows. The rate of the temperature-field variation at the transient heat transfer in the solid phase is determined by value of its thermal diffusivity $\alpha = k/(\rho c_p)$, where ρ is density [$\text{kg}\cdot\text{m}^{-3}$]; c_p is specific heat capacity [$\text{kJ}\cdot\text{kg}^{-1}\cdot\text{K}^{-1}$]. The measurement of the PW and PW/EG#2 caloric properties [19] showed the decreasing both the specific isobaric heat

capacity of the liquid phase by 10–16% and the total phase-transition enthalpy by 15–21% for the PW containing the 0.111 g·g⁻¹ of EG *vs.* pure PW. That is, increasing the content of EG contributes to both the increasing the thermal conductivity and the decreasing the caloric properties of the composite PCM.

Based on discussed results, it can be stated the feasibility of future studying the prospects of using EG as additives to the PW. Further studies of the rational content of the EG in PW are required (the fraction of EG in PCM may be different depending on their application). It should also be noted the necessity of developing a general criterion that combines both technological characteristics of the PCM (its thermophysical properties and the rates of heating and cooling of the capsules with PCM) as well as economic factors. In addition, the possibility of the CFD simulation of the processes for charging and discharging a capsule filled with composite PCMs containing EG based on using its thermophysical properties remains unclear. This question also needs further examination.

5. CONCLUSIONS

This study assesses the feasibility of utilizing the composite PW-based PCM containing the EG in the TES system. For this purpose, a comprehensive experimental study of the effect of EG on the PW thermophysical properties and the rate of changing its temperature during heating and cooling was performed. The following conclusion can be formulated based on the results obtained:

- two samples of PW-based composite PCM were prepared using different methods: PW/EG#1 containing 0.178 g·g⁻¹ of EG (preparing without evacuation of the components) and PW/EG#2 with 0.111 g·g⁻¹ of EG (preparing with components' evacuation); the evacuation process provides more complete filling of the EG pores with PW and less content of EG in PCM (air content in PW/EG#1 was of 7.50 vol.% *vs.* 4.75 vol.% in PW/EG#2);
- the densities of PW/EG#1 and PW/EG#2 are greater than the PW density, but their variation does not correspond to additivity rule; it was not observed the 'jump' of the density for PW-containing EG during the transition of the PW melting point;
- the thermal conductivity average value of solid phase (20–50°C) for the PW/EG#1 and PW/EG#2 is increased by 800% and 640%, respectively, compared to the pure PW; enhancement of the thermal conductivity for PW/EG#1 and PW/EG#2 in the range above PW melting point (60–70°C) was of 930% and 740%, respectively, compared to the pure PW.
- the melting and heating duration from 48°C to 59°C for the PW in model of the capsule TES system was of about 12.0 minutes *vs.*

about 1.1 and 1.4 minutes for the PW/EG#1 and PW/EG#2, respectively; the heating duration from 30 to 40°C for the PW was of about 7.7 minutes *vs.* about 1.6 minutes for both PW/EG#1 and PW/EG#2; the main heat-transfer mechanism in PW/EG is thermal conductivity through the EG skeleton; the bottom-up convective currents of liquid PW are absent; this fact will contribute to the faster smoothing of the temperature field of capsules with PCM PW/EG in TES systems;

— the increase in the EG mass fraction in the PW leads to enhancement of the composite PCM thermal conductivity, but does not lead to a significant increase in the heating and cooling rates of the capsule with the PCM; the obtained effect is explained by deterioration of the caloric properties for the composite PCM with increasing content of the EG; selection of the rational EG mass fraction in the PW to obtain the effective composite PCM for the TES requires further investigation.

ACKNOWLEDGMENT

The authors are grateful to the National Research Foundation of Ukraine (project No. 2020.02/0125) for financial support of this study.

REFERENCES

1. S. Rostami, M. Afrand, A. Shahsavari, M. Sheikholeslami, R. Kalbasi, S. Aghakhani, S. Shadloo, and H. F. Oztop, *Energy*, **211**: 118698 (2020); <https://doi.org/10.1016/j.energy.2020.118698>
2. M. Li, and B. Mu, *Appl. energy*, **242**: 695 (2019); <https://doi.org/10.1016/j.apenergy.2019.03.085>
3. Z. A. Qureshi, H. M. Ali, and S. Khushnood, *Int. J. Heat Mass Transfer*, **127**, Part C: 838 (2018); <https://doi.org/10.1016/j.ijheatmasstransfer.2018.08.049>
4. P. Cheng, X. Chen, H. Gao, X. Zhang, Z. Tang, A. Li, and G. Wang, *Nano Energy*, **85**: 105948 (2021); <https://doi.org/10.1016/j.nanoen.2021.105948>
5. X. Py, R. Olives, and S. Mauran, *Int. J. Heat Mass Transfer*, **44**, No. 14: 2727 (2001); [https://doi.org/10.1016/S0017-9310\(00\)00309-4](https://doi.org/10.1016/S0017-9310(00)00309-4)
6. A. Sari and A. Karaipekli, *Appl. Therm. Eng.*, **27**, Iss. 8–9: 1271 (2007); <https://doi.org/10.1016/j.applthermaleng.2006.11.004>
7. Z. P. Liu, and R. Yang, *Appl. Sci.*, **7**, No. 6: 574 (2017); <https://doi.org/10.3390/app7060574>
8. M. Kenisarin, K. Mahkamov, F. Kahwash, and I. Makhkamova, *Sol. Energy Mater. Sol. Cells*, **200**: 110026 (2019); <https://doi.org/10.1016/j.solmat.2019.110026>
9. Y. Zhao, L. Jin, B. Zou, G. Qiao, T. Zhang, L. Cong, F. Jiang, C. Li, Y. Huang, and Y. Ding, *Appl. Therm. Eng.*, **171**: 115015 (2020);

- <https://doi.org/10.1016/j.applthermaleng.2020.115015>
10. X. L. Wang, B. Li, Z. G. Qu, J. F. Zhang, and Z. G. Jin, *Int. J. Heat Mass Transfer*, **155**: 119853 (2020);
<https://doi.org/10.1016/j.ijheatmasstransfer.2020.119853>
 11. X. Hu, H. Wu, X. Lu, S. Liu, and J. Qu, *Adv. Compos. Hybrid Mater.*, **4**: 478 (2021); <https://doi.org/10.1007/s42114-021-00300-6>
 12. Y. Liang, Z. Tao, Q. Guo, and Z. Liu, *Journal of Energy Storage*, **39**: 102634 (2021); <https://doi.org/10.1016/j.est.2021.102634>
 13. G. Fang, M. Yu, K. Meng, F. Shang, and X. Tan, *Energy Fuels*, **34**, No. 8: 10109 (2020); <https://doi.org/10.1021/acs.energyfuels.0c00955>
 14. D. Elwell, R. S. Feigelson, and G. M. Rao, *J. Electrochem. Soc.*, **130**, Iss. 5: 1021 (1983); <https://doi.org/10.1149/1.2119877>
 15. I. Y. Sementsov, G. P. Prikhodko, S. L. Revo, A. V. Melezhyk, M. L. Pyatkovskiy, and V. V. Yanchenko, *Hydrogen Mater. Sci. Chem. Carbon Nanomater. NATO Science Series II: Mathematics, Physics and Chemistry* (Dordrecht: Springer: 2004), vol. **172**; https://doi.org/10.1007/1-4020-2669-2_47
 16. K. Sever, I. H. Tavman, Y. Seki, A. Turgut, M. Omastova, and I. Ozdemir, *Composites. Part B*, **53**: 226 (2013);
<https://doi.org/10.1016/j.compositesb.2013.04.069>
 17. M. Krzesińska, *Mater. Chem. Phys.*, **87**, Iss. 2–3: 336 (2004);
<https://doi.org/10.1016/j.matchemphys.2004.05.030>
 18. O. Khliyeva, V. Zhelezny, A. Nikulin, M. Lapardin, D. Ivchenko, and E. Palomo del Barrio, *Proc. 11th Int. Conf. 'Nanomaterials: Applications & Properties' (September 5–11, 2021, Odesa, Ukraine)*, TPNS04-2;
<https://doi.org/10.1109/NAP51885.2021.9568522>
 19. Ya. Hlek, O. Khliyeva, D. Ivchenko, N. Lapardin, V. Khalak, and V. Zhelezny, *Nanosistemi, Nanomateriali, Nanotehnologii*, **20**, Iss. 3: 741 (2022); <https://doi.org/10.15407/nnm.20.03.745>
 20. O. Khliyeva, V. Zhelezny, A. Paskal, Ya. Hlek, and D. Ivchenko, *East-Eur. J. Enterp. Technol.*, **4**, No. 5 (112): 12 (2021);
<https://doi.org/10.15587/1729-4061.2021.239065>
 21. A. Sarı and A. Karaipekli, *Appl. Therm. Eng.*, **27**, Iss. 8–9: 1271 (2007);
<https://doi.org/10.1016/j.applthermaleng.2006.11.004>
 22. S. Tao, S. Wei, and Y. Yulan, *J. Mater. Civ. Eng.*, **27**, Iss. 4: 04014156 (2015); [https://doi.org/10.1061/\(ASCE\)MT.1943-5533.0001089](https://doi.org/10.1061/(ASCE)MT.1943-5533.0001089)
 23. L. Xia, P. Zhang, and R. Z. Wang, *Carbon*, **48**, Iss. 9: 2538 (2010);
<https://doi.org/10.1016/j.carbon.2010.03.030>
 24. N. Ukrainczyk, S. Kurajica, and J. Šipušić, *Chem. Biochem. Eng. Q.*, **24**, No. 2: 129 (2010).
 25. A. F. Elmozughi, L. Solomon, A. Oztekin, and S. Neti, *Int. J. Heat Mass Transfer*, **78**: 1135 (2014);
<https://doi.org/10.1016/j.ijheatmasstransfer.2014.07.087>
 26. A. Abhat, *Sol. Energy*, **30**, Iss. 4: 313 (1983); [https://doi.org/10.1016/0038-092X\(83\)90186-X](https://doi.org/10.1016/0038-092X(83)90186-X)
 27. S. Motahar and R. Khodabandeh, *Trans. Phenom. Nano Micro Scales*, **6**, Iss. 2: 96 (2018); <https://doi.org/10.22111/tpnms.2018.22225.1133>
 28. S. Motahar, N. Nikkam, A. A. Alemrajabi, R. Khodabandeh, M. S. Toprak, and M. Muhammed, *Int. Commun. Heat Mass Transfer*, **56**: 114 (2014);

- <https://doi.org/10.1016/j.icheatmasstransfer.2014.06.005>
29. L. Klintberg, M. Svedberg, F. Nikolajeff, and G. Thornell, *Sens. Actuators. A*, **103**, Iss. 3: 307 (2003); [https://doi.org/10.1016/S0924-4247\(02\)00403-X](https://doi.org/10.1016/S0924-4247(02)00403-X)
 30. J. DeSain, B. Brady, K. Metzler, T. Curtiss, and T. Albright, 45th *AIAA/ASME/SAE/ASEE Jt. Propuls. Conf. Exhib. (August 2–5, 2009, Denver, CO, USA)*; <https://doi.org/10.2514/6.2009-5115>
 31. F. O. Al Ghuol, K. Sopian, and S. Abdullah, *Journal of Thermodynamics*, **2016**: 1604782 (2016); <https://doi.org/10.1155/2016/1604782>
 32. J. Wang, H. Xie, and Z. Xin, *Thermochim. Acta*, **488**, Iss. 1–2: 39 (2009); <https://doi.org/10.1016/j.tca.2009.01.022>
 33. P. Stephan, S. Kabelac, M. Kind, H. Martin, D. Mewes, and K. Schaber, *VDI Heat Atlas* (Springer: 2010), p. 1585.